

## IMPROVING PRECIPITATION FORECASTS BY THE OPERATIONAL NONHYDROSTATIC MESOSCALE MODEL WITH THE KAIN-FRITSCH CONVECTIVE PARAMETERIZATION AND CLOUD MICROPHYSICS

Masami Narita\* and Shiro Ohmori  
Japan Meteorological Agency, Otemachi, Tokyo, Japan

### 1. INTRODUCTION

The Japan Meteorological Agency (JMA) has operated a nonhydrostatic mesoscale model (MSM) of 10-km horizontal grid spacing (10-km MSM) since September 2004 (Saito et al. 2006). The horizontal grid spacing has been enhanced to 5 km (5-km MSM) since March 2006 and the forecast time has been extended from 15 hours to 33 hours at the initial times of 03, 09, 15, 21 UTC with some modifications including dynamics and physics schemes since June 2007 (Saito et al. 2007).

The development of a moist process scheme to improve precipitation forecasts is continued since the major purpose of MSM is to prevent natural disasters such as torrential rain. Preliminary forecast tests of 10-km MSM with only cloud microphysics sometimes indicated the necessity of a convective parameterization scheme in order that the stability of time integration is assured and that weak precipitation of forecasts matches well with that of observations. To accomplish these aims, the Kain-Fritsch (KF) convective parameterization scheme was adopted simultaneously with a cloud microphysics scheme to MSM. As Molinari and Dudek (1992) indicated the uncertainty of treatment of convection for grid spacing from about 3 km to 20-25 km, formation of line-shaped mesoscale rainband was sometimes simulated better with only cloud microphysics without convective parameterization. According to the several forecasts, however, it became clear that the average objective scores for the precipitation forecasts by MSM with convective parameterization and cloud microphysics were better than those with only cloud microphysics. This fact is considered to be an important characteristic as an operational numerical prediction model.

To improve precipitation forecasts by 10-km MSM and 5-km MSM with the KF scheme, some modifications to formulation of precipitation and

triggering of convection were added to the original KF scheme and parameters were adjusted. As a result, the forecast skill was quite improved compared to pre-operational MSM from the viewpoint of quantitative precipitation forecasts.

Full configurations of 10-km MSM and 5-km MSM can be found in Saito et al. (2007). In this paper, the configuration of a cloud microphysics parameterization scheme is summarized in section 2. Some modifications to the KF scheme with operational MSM and their effects are presented in section 3. Section 4 provides conclusions.

### 2. CLOUD MICROPHYSICS

A bulk parameterization scheme of cloud microphysics based on Lin et al. (1983) has been adopted to the original root of MSM developed at the Forecast Research Department of the Meteorological Research Institute (Ikawa and Saito 1991). In this scheme, water substance is expressed by its mixing ratio and categorized into six forms: water vapor, cloud water, rain, cloud ice, snow and graupel. Although the original cloud microphysics scheme predicts the number concentrations of cloud ice, snow and graupel (Murakami 1990), operational MSM predicts only the mixing ratios. Furthermore, some simplification and elimination of the original cloud microphysics scheme were applied in order to shorten the computational time without making precipitation forecasts worse (Yamada 2003).

The prognostic equations for mixing ratios of six water substances ( $q_v$ : water vapor,  $q_c$ : cloud water,  $q_r$ : rain,  $q_i$ : cloud ice,  $q_s$ : snow,  $q_g$ : graupel) and potential temperature ( $\theta$ ) are as follows:

$$\begin{aligned} & \frac{\partial q_v}{\partial t} + \text{ADV}(q_v) - \text{DIF}(q_v) \\ &= P_{v\_evp\_r} - P_{i\_dep\_v} - P_{s\_dep\_v} - P_{g\_dep\_v} \\ & \quad - P_{i\_nud\_v} - P_{w\_cnd\_v}, \end{aligned}$$

$$\begin{aligned} & \frac{\partial q_c}{\partial t} + \text{ADV}(q_c) - \text{DIF}(q_c) \\ &= -P_{r\_aut\_w} - P_{r\_ac\_r\_w} + P_{w\_cnd\_v} - P_{i\_frz\_w} \\ & \quad - P_{s\_ac\_s\_w} - P_{g\_ac\_s\_w} - P_{g\_ac\_g\_w} \\ & \quad + \delta P_{w\_mlt\_i}, \end{aligned}$$

---

\* *Corresponding author address*: Masami Narita, Numerical Prediction Division, Japan Meteorological Agency, 1.3.4 Otemachi, Chiyodaku, Tokyo 100-8122, Japan  
E-mail: m\_narita@naps.kishou.go.jp

$$\begin{aligned}
& \frac{\partial q_r}{\partial t} + \text{ADV}(q_r) - \text{DIF}(q_r) \\
& = -P_{\text{prc}_r} + \text{Pr}_{\text{ac}_r_w} + \text{Pr}_{\text{aut}_w} - \text{Pv}_{\text{evp}_r} \\
& \quad - \text{Pg}_{\text{frz}_r} - \text{Pg}_{\text{ac}_i_r} - \text{Ps}_{\text{ac}_s_r} - \text{Pg}_{\text{ac}_s_r} \\
& \quad - \text{Pg}_{\text{ac}_g_r} + \delta (\text{Pr}_{\text{mlt}_s} + \text{Pr}_{\text{mlt}_g}), \\
& \frac{\partial q_i}{\partial t} + \text{ADV}(q_i) - \text{DIF}(q_i) \\
& = \text{Pi}_{\text{nud}_v} + \text{Pi}_{\text{frz}_w} + \text{Pi}_{\text{dep}_v} - \text{Pg}_{\text{ac}_r_i} \\
& \quad - \text{Ps}_{\text{ac}_s_i} - \text{Pg}_{\text{ac}_g_i} - \text{Ps}_{\text{aut}_i} - \delta \text{Pw}_{\text{mlt}_i}, \\
& \frac{\partial q_s}{\partial t} + \text{ADV}(q_s) - \text{DIF}(q_s) \\
& = -P_{\text{prc}_s} + \text{Ps}_{\text{dep}_v} + \text{Ps}_{\text{aut}_i} + \text{Ps}_{\text{ac}_s_w} \\
& \quad - \text{Pg}_{\text{cn}_w_s} + \text{Ps}_{\text{ac}_s_i} + \text{Ps}_{\text{ac}_s_r} - \text{Pg}_{\text{ac}_r_s} \\
& \quad - \text{Pg}_{\text{ac}_g_s} - \delta \text{Pr}_{\text{mlt}_s}, \\
& \frac{\partial q_g}{\partial t} + \text{ADV}(q_g) - \text{DIF}(q_g) \\
& = -P_{\text{prc}_g} + \text{Pg}_{\text{dep}_v} + \text{Pg}_{\text{cn}_w_s} + \text{Pg}_{\text{ac}_s_w} \\
& \quad + \text{Pg}_{\text{ac}_g_r} + \text{Pg}_{\text{ac}_g_s} + \text{Pg}_{\text{ac}_g_w} + \text{Pg}_{\text{ac}_g_i} \\
& \quad + \text{Pg}_{\text{ac}_i_r} + \text{Pg}_{\text{ac}_r_i} + \text{Pg}_{\text{ac}_s_r} + \text{Pg}_{\text{ac}_r_s} \\
& \quad + \text{Pg}_{\text{frz}_r} - \delta \text{Pr}_{\text{mlt}_g}, \\
& \frac{\partial \theta}{\partial t} + \text{ADV}(\theta) - \text{DIF}(\theta) \\
& = -\frac{L_v}{c_p \pi} (\text{Pv}_{\text{evp}_r} - \text{Pw}_{\text{cnd}_v}) \\
& \quad + \frac{L_s}{c_p \pi} (\text{Pi}_{\text{dep}_v} + \text{Pi}_{\text{nud}_v} + \text{Ps}_{\text{dep}_v} + \text{Pg}_{\text{dep}_v}) \\
& \quad + \frac{L_f}{c_p \pi} (\text{Ps}_{\text{ac}_s_w} + \text{Pg}_{\text{ac}_s_w} + \text{Pg}_{\text{ac}_g_w}) \\
& \quad + \frac{L_f}{c_p \pi} (\text{Pg}_{\text{ac}_i_r} + \text{Pi}_{\text{frz}_w}) \\
& \quad + \frac{L_f}{c_p \pi} (\text{Ps}_{\text{ac}_s_r} + \text{Pg}_{\text{ac}_s_r} + \text{Pg}_{\text{ac}_g_r}) \\
& \quad - \delta \frac{L_f}{c_p \pi} (\text{Pw}_{\text{mlt}_i} + \text{Pr}_{\text{mlt}_s} + \text{Pr}_{\text{mlt}_g}),
\end{aligned}$$

where  $t$  is time,  $\text{ADV}(x)$  the advection term of  $x$  and  $\text{DIF}(x)$  the diffusion term of  $x$ . The symbols  $L_v$ ,  $L_s$  and  $L_f$  are latent heat of vaporization, sublimation and fusion, respectively;  $c_p$  the specific heat of dry air at constant pressure,  $\pi$  the non-dimensional pressure (Exner function), and  $\delta = 1$  when the temperature is above 0 deg C and  $\delta = 0$  otherwise. The symbol  $Px_{\text{proc}_y}$  denotes the production rate of water substance  $x$  ( $v$ : water vapor,  $w$ : cloud water,  $r$ : rain,  $i$ : cloud ice,  $s$ : snow,  $g$ : graupel) through the process  $\text{proc}$  ( $ac$ : accretion,  $aut$ : autoconversion,  $cn$ : conversion such as riming,  $cnd$ : condensation,  $dep$ : depositional growth or evaporation,  $evp$ : evaporation,  $frz$ : freezing,  $mlt$ : melting,  $nud$ : nucleation (by deposition) concerning water substance  $y$ ,  $Px_{\text{proc}_y_z}$  denotes the

production rate of water substance  $x$  through the process  $\text{proc}$  concerning water substances  $y$  and  $z$ , and  $P_{\text{prc}_x}$  denotes precipitation of  $x$ .

### 3. MODIFICATIONS TO THE KAIN-FRITSCH CONVECTIVE PARAMETERIZATION SCHEME

The Kain-Fritsch convective parameterization scheme (Kain and Fritsch 1990; Kain 2004) is adopted to represent the effects of subgrid-scale convection. The source codes of the KF scheme have been originally developed for the Weather Research and Forecast (WRF) modeling system and implemented to MSM with Dr. Kain's consent in April 2002. Minor improvements for the original KF scheme made before February 2003 have also been reflected. Some modifications and adjustments were applied to the KF scheme in MSM.

During the pre-operational forecast tests, the area of precipitation predicted by MSM with only cloud microphysics was sometimes too narrow, and moreover observed precipitation was sometimes missed. With the KF scheme, these weaknesses were improved. As shown in Fig. 1, distribution of accumulated precipitation forecast by 5-km MSM with only cloud microphysics is insufficient especially over northern area of Japan and its surrounding sea compared to that with convective parameterization and cloud microphysics.

Some modifications and adjustments to the KF scheme and their effects are presented here.

#### 3.1 Trigger function

To identify source layers for convective clouds, the KF scheme utilizes a trigger function based on the temperature at the lifting condensation level (LCL) and the grid-scale vertical velocity (Fritsch and Chappell 1980; Kain 2004). The temperature perturbation based on the vertical velocity is given by

$$\Delta T_{\text{LCL}} = \left( \overline{w}_{\text{LCL}} \frac{\Delta x}{25000} - w_{\text{zLCL}} \right)^{\frac{1}{3}},$$

where  $\overline{w}_{\text{LCL}}$  is a grid-scale vertical velocity at the LCL,  $\Delta x$  is a grid spacing, and

$$w_{\text{zLCL}} = \begin{cases} w_0 \frac{z_{\text{LCL}}}{2000}, & \text{if } z_{\text{LCL}} \leq 2000 \text{ m} \\ w_0, & \text{if } z_{\text{LCL}} > 2000 \text{ m} \end{cases}$$

where  $w_0 = 0.02 \text{ ms}^{-1}$  and  $z_{\text{LCL}}$  is a height of the LCL.

While the vertical velocity  $\overline{w}_{\text{LCL}}$  of one model grid is adopted as a temperature perturbation  $\Delta T_{\text{LCL}}$

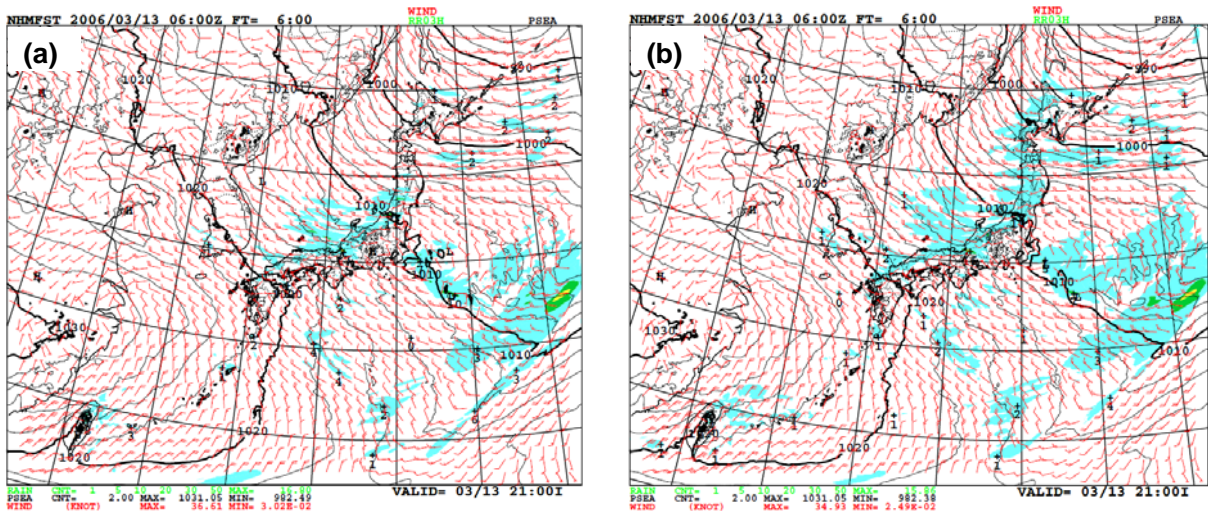


Fig. 1. Accumulated precipitation [mm/3h] from 09-12 UTC on 13<sup>th</sup> March 2006.  
 (a) 6-hour forecast by 5-km MSM with only cloud microphysics.  
 (b) Same as (a) but with the Kain-Fritsch convective parameterization scheme and cloud microphysics.

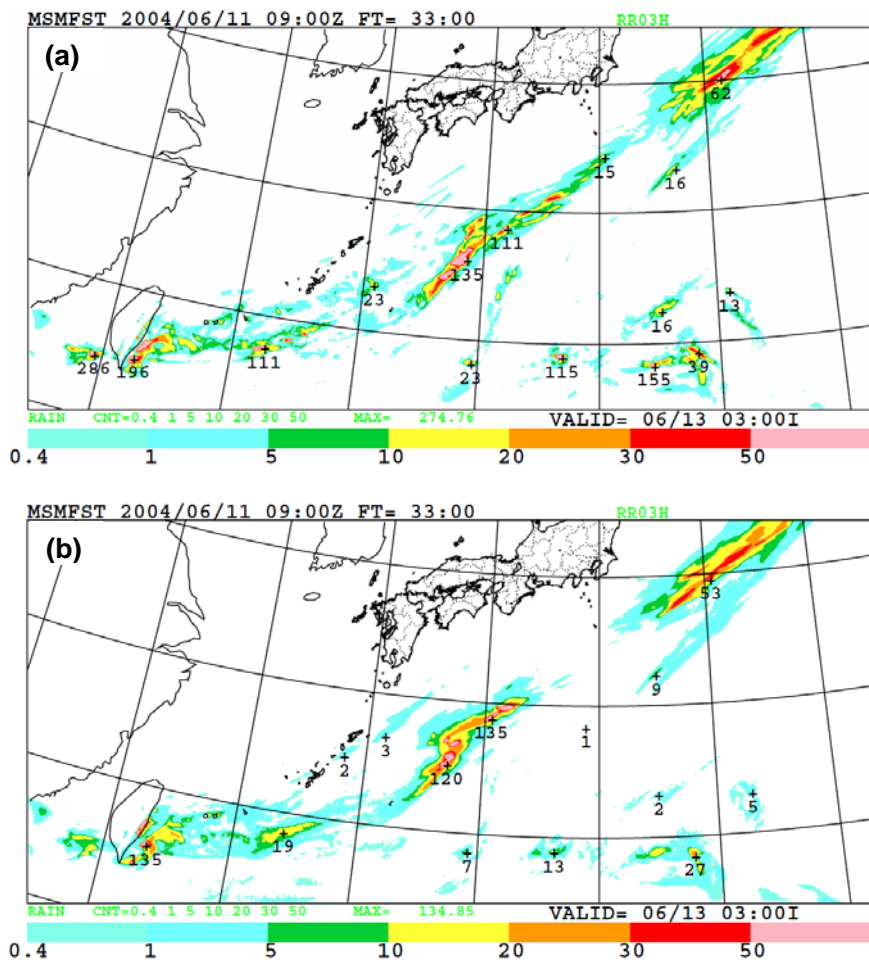


Fig. 2. Accumulated precipitation [mm/3h] from 15-18 UTC on 12<sup>th</sup> June 2004.  
 (a) 33-hour forecast by 5-km MSM with the KF scheme without relative humidity based perturbation.  
 (b) Same as (a) but with relative humidity based perturbation.

for the KF scheme in the WRF model, the horizontally-averaged vertical velocity of the grid and surrounding eight grids is adopted as  $\bar{w}_{LCL}$  in operational MSM to eliminate an influence of the grid-scale intensified vertical velocity. Even though this temperature perturbation is formulated as a function of horizontal grid spacing, a value calculated with original formulation may be too large for MSM with 5-km or 10-km horizontal grid spacing and causes sometimes undesirable precipitation in regions where no precipitation was observed. Thus, the temperature perturbation depending on the vertical velocity is reduced by a certain amount of the values determined in the original formulation.

The original KF scheme applied to the humid climate area of Japan and its surrounding sea sometimes fails to initiate parameterized convection when the lowest atmosphere is wet and dynamical forcing is weak. To eliminate this weakness, a temperature perturbation based on the relative humidity has been added to the trigger function. The temperature perturbation based on the relative humidity has been implemented for the High Resolution Limited Area Model (HIRLAM, Uden et al. 2002) and is given by

$$\Delta T_{vRH} = \begin{cases} 0, & \text{if } R_{hLCL} < 0.75 \\ \frac{0.25(R_{hLCL} - 0.75)Q_{mix}}{\partial Q_{SLCL}/\partial T}, & \text{if } 0.75 \leq R_{hLCL} \leq 0.95 \\ \frac{(1/R_{hLCL} - 1)Q_{mix}}{\partial Q_{SLCL}/\partial T}, & \text{if } R_{hLCL} > 0.95 \end{cases}$$

where  $R_{hLCL}$  is the relative humidity at the LCL,  $T$  is the temperature,  $Q_{SLCL}$  is the saturation mixing ratio at the LCL,  $Q_{mix}$  is the mixing ratio of updraft

source layer. The temperature perturbation is reduced a certain amount of the value determined by the formulation of Uden et al. (2002) in 5-km MSM.

Figure 2 shows accumulated precipitation forecasts by 5-km MSM. According to Fig. 2 (a) by 5-km MSM with the original KF scheme, too narrow and too intensified precipitation was calculated at the western sea of Taiwan (286 mm/3h), southern sea of Okinawa island (111 mm/3h) and so on. On the other hand, too intensified precipitation caused by grid-point storm was eliminated by 5-km MSM with the modified KF scheme as shown in Fig. 2 (b).

Inclusion of the temperature perturbation depending on the relative humidity also improved the forecast of diurnal convective rain. Figure 3 shows an example of precipitation forecasts by 5-km MSM with the original and modified KF schemes. Even though the amount of precipitation was not enough compared to observation, accumulated precipitation forecasted by the modified KF scheme was better than that by the original KF scheme.

### 3.2 Precipitation formation

In the original KF scheme, precipitation is continuously produced in convective updraft regardless of the content of condensate by a method proposed by Ogura and Cho (1973). As shown in Fig. 4 (b), the formation of precipitation by 10-km MSM with the original KF scheme sometimes produces unnatural distribution such as elongated regions whose orientations are perpendicular to major rainbands observed by radar and rain gauge as shown in Fig. 4 (a). To eliminate this weakness, the method for calculation of precipitation is replaced by the Kessler-type autoconversion scheme in the modified KF scheme. In this scheme, precipitation formation is adopted such that condensate in convective updraft is converted into precipitation when its amount exceeds

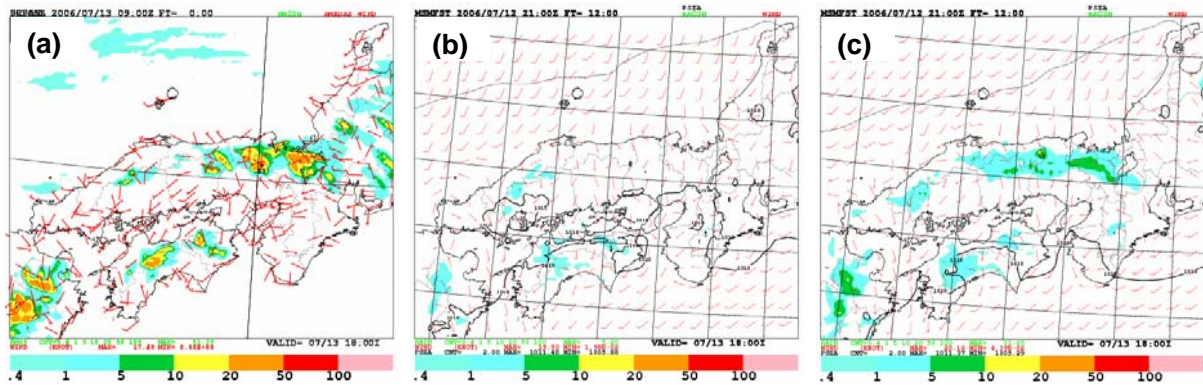


Fig. 3. Accumulated precipitation [mm/3h] from 06-09 UTC on 13<sup>th</sup> July 2006.

- (a) Observation (derived from radar data corrected by rain gauge data).
- (b) 33-hour forecast by 5-km MSM with the KF scheme without relative humidity based perturbation.
- (c) Same as (a) but with relative humidity based perturbation.

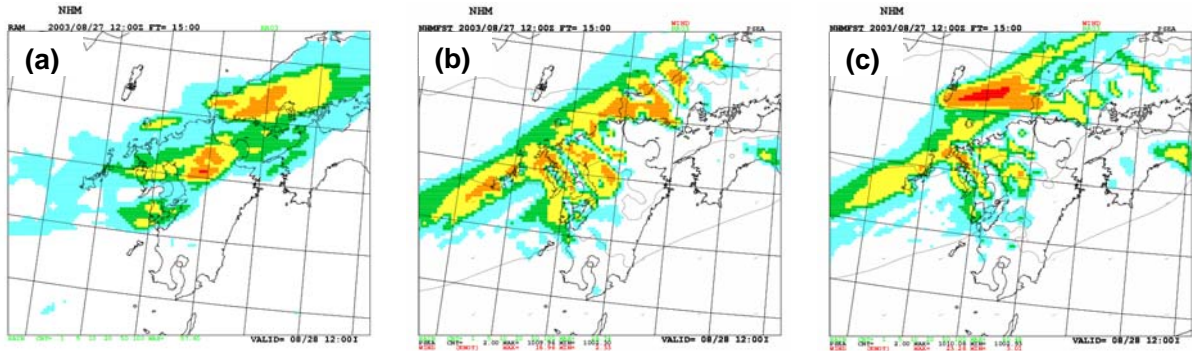


Fig. 4. Accumulated precipitation [mm/3h] from 00-03 UTC on 28<sup>th</sup> August 2003.  
 (a) Observation (derived from radar data corrected by rain gauge data).  
 (b) 15-hour forecast by 10-km MSM with the original KF scheme.  
 (c) Same as (b) but with the Kessler-type autoconversion.

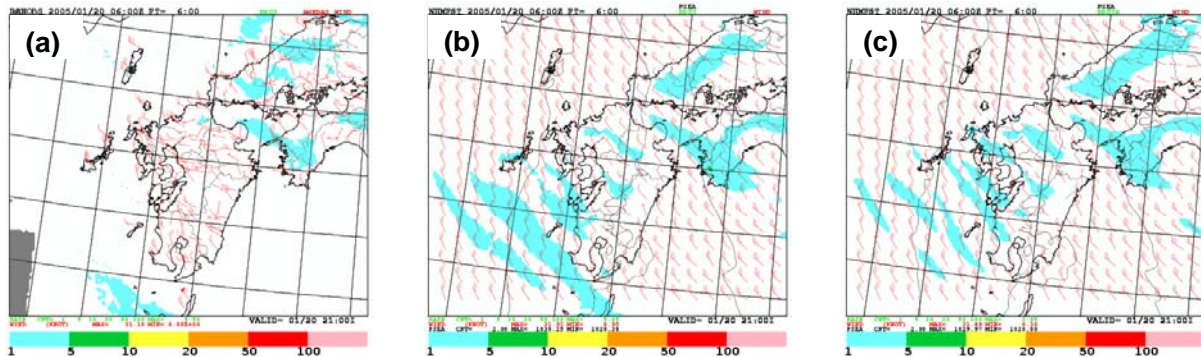


Fig. 5. Accumulated precipitation [mm/3h] from 09-12 UTC on 20<sup>th</sup> January 2005.  
 (a) Observation (derived from radar data corrected by rain gauge data).  
 (b) 6-hour forecast by 5-km MSM with the original KF scheme, time scale for shallow convection = 2400 seconds.  
 (c) Same as (b) but time scale for shallow convection = 600 seconds.

a threshold value. As shown in Fig. 4 (c), the unnatural distribution of accumulated precipitation is eliminated by the modified KF scheme.

The threshold value  $8.0 \times 10^{-4} \text{ kg kg}^{-1}$  in 10-km MSM is increased to  $1.0 \times 10^{-3} \text{ kg kg}^{-1}$  in 5-km MSM to eliminate precipitation calculated by the KF scheme and to improve the representation of weak precipitation in summer season.

### 3.3 Time scale for convection

The KF scheme assumes that the convection consumes the convective available potential energy (CAPE) in a certain time scale. This time scale, within 1800 to 3600 seconds, is based on the advective time scale and is used to determine the heating and moistening ratios. The original formulation of the KF scheme assigns this time scale of 1800 seconds for a fine mesh model with horizontal grid spacing less than 10 km. A shorter time scale of 900 seconds improves the precipitation forecast by rain rate frequency.

The importance of the time scale for shallow convection is appeared in the precipitation forecasts during the cold air outbreak of winter monsoon. Under this condition, shallow convective clouds developed over the sea bring about precipitation. With a value of 2400 seconds assigned for the original formulation, the band-shaped weak rain is sometimes excessively produced. With a shorter time scale of 600 seconds, the excess weak precipitation is ameliorated well as shown in figure 5.

## 4. CONCLUSIONS

An operational nonhydrostatic mesoscale model of 10-km and 5-km horizontal grid spacing with cloud microphysics and the Kain-Fritsch convective parameterization scheme has been developed at the Japan Meteorological Agency. The result of pre-operational forecast tests with only cloud microphysics showed some weaknesses. On the other hand, the forecast scores for precipitation were improved by the Kain-Fritsch scheme with some

modifications to formulation of precipitation and triggering of convection.

## REFERENCES

Fritsch, J. M., and C. F. Chappell, 1980: Numerical prediction of convectively driven mesoscale pressure systems. Part I: Convective parameterization. *J. Atmos. Sci.*, **37**, 1722-1733.

Ikawa, M. and K. Saito, 1991: Description of a non-hydrostatic model developed at the Forecast Research Department of the MRI. *MRI Tech. Rep.* **28**, 238 pp.

Kain, J. S., 2004: The Kain-Fritsch convective parameterization: An update. *J. Appl. Meteor.*, **43**, 170-181.

Kain, J. S., and J. M. Fritsch, 1990: A one-dimensional entraining/detraining plume model and its application in convective parameterization. *J. Atmos. Sci.*, **47**, 2784-2802.

Lin, Y. -L., R. D. Farley and H. D. Orville, 1983: Bulk parameterization of the snow field in a cloud model. *J. Climate Appl. Meteor.*, **22**, 1065-1092.

Molinari, J., and M. Dudek, 1992: Parameterization of convective precipitation in mesoscale numerical models: A critical review. *Mon. Wea. Rev.*, **120**, 326-344.

Murakami, M., 1990: Numerical modeling of dynamical and microphysical evolution of an isolated convective cloud - the 19 July 1981 CCOPE cloud. *J. Meteor. Soc. Japan*, **68**, 107-128.

Ogura, Y., and H. -R. Cho, 1973: Diagnostic determination of cumulus cloud populations from observed large-scale variables. *J. Atmos. Sci.*, **30**, 1276-1286.

Saito, K., T. Fujita, Y. Yamada, J. Ishida, Y. Kumagai, K. Aranami, S. Ohmori, R. Nagasawa, S. Kumagai, C. Muroi, T. Kato, H. Eito, and Y. Yamazaki, 2006: The operational JMA nonhydrostatic model. *Mon. Wea. Rev.*, **134**, 1266-1298.

Saito, K., J. Ishida, K. Aranami, T. Segawa, M. Narita, and Y. Honda, 2007: Nonhydrostatic atmospheric models and operational development at JMA. *125<sup>th</sup> anniversary issue of the Journal of the Meteorological Society of Japan*. (Submitted)

Undén, P., L. Rontu, H. Järvinen, P. Lynch, J. Calvo, G. Cats, J. Cuxart, K. Eerola, C. Fortelius, J. A. Garcia-Moya, C. Jones, G. Lenderlink, A. McDonald, R.

McGrath, B. Navascues, N. W. Nielsen, V. Ødegaard, E. Rodriguez, M. Rummukainen, R. Rööf, K. Sattler, B. H. Sass, H. Savijärvi, B. W. Schreur, R. Sigg, H. The, A. Tijm, 2002: *HIRLAM-5 Scientific Documentation*, pp.144.

Yamada, Y., 2003: Cloud microphysics. *Separate volume of annual report of Numerical Prediction Division/Japan Meteorological Agency*, **49**, 52-76. (in Japanese)